CDF note 8701

Search for charged, massive stable particles

The CDF Collaboration
URL http://www-cdf.fnal.gov
(Dated: February 18, 2007)

Under some circumstances, new massive particles arising from physics beyond the Standard Model will have lifetimes that are long compared to the transit time through the CDF detector. In these cases, direct searches for decay products will fail, and the limits obtained will not hold. If such a particle is charged, it will appear in the detector as a slowly-moving, highly-ionizing and highly penentrating particle with large transverse momentum that will typically be reconstructed as a muon. We present the results of a model-independent search for charged massive stable particles (CHAMPs) by measuring the time-of-flight of high transverse momentum tracks in events collected using a high transverse momentum muon trigger. Our results, based upon 1.03 fb^{-1} of pbar-p collisions at $\sqrt{s} = 1.98$ TeV, are consistent with background. We set a model independent limit on the production cross section of a single fiducial strongly interacting CHAMP of 48 fb at 95% C.L., and 10 fb for a weakly-interacting CHAMP. Within the context of a general model of stable stop pair production, we set a lower stop mass limit of 250 GeV/c^2 at 95% C.L.

Preliminary Results for Winter 2007 Conferences

I. INTRODUCTION

The discovery and characterization of new particles will provide one of the most important clues to the nature of physics beyond the Standard Model. While most searches for such particles assume that any new massive particle will decay promptly within the detector, it is possible that the states most accessible to the Tevatron experiments are stable due to the existence of a new symmetry [1], a weak coupling to the decay mechanism [2] or a kinematic constraint [3]. If the resulting lifetime is comparable to the typical transit time through the detector, then the particles may escape the detector, thereby evading the limits imposed by direct searches for decay products. If such a particle is charged, however, it will be directly observable within the detector and present a distinctive signature, that of a slowly-moving, high transverse momentum ($p_{\rm t}$) particle. The low velocity results in a long time-of-flight and an anomalously large dE/dx. Since the particles typically lose energy primarily through ionization [4][5], they will be highly penetrating and will likely be reconstructed as muons.

Non-accelerator experiments have ruled out the existence of CHAMPs that have a mass below about 230 GeV/c^2 and that have lifetimes on the time scale of the age of the oceans [6]. The same data excludes CHAMPs with a mass less than about 1 TeV/c^2 and with a lifetime on the scale of the age of the universe, although the limit depends critcally upon certain details of the thermal history of the universe. In Run 1, CDF placed lower limits of 190 GeV/c^2 on a stable down-like fourth generation quark, and 220 GeV/c^2 on a stable up-like quark based upon a search for highly ionizing particles with large $p_{\rm t}$ [7]. The ALEPH experiment also used dE/dx to set a lower limit of 95 GeV/c^2 on a stable stop squark [8]. Stable sleptons have been excluded below a mass of about 99.5 GeV/c^2 based upon the combined results from the LEP2 experiments [9].

We present here the results of a model-independent search for charged massive stable particles (CHAMPs) produced in $\bar{p}p$ collisions at $\sqrt{s} = 1.98$ TeV with the CDF detector at the Fermilab Tevatron. The analysis is based upon an integrated luminosity of 1.03 fb^{-1} collected using a high-$p_{\rm t}$ muon trigger. This signature-based search isolates heavy, high-$p_{\rm t}$ particles by using the measured velocity and momentum of the particle to calculate the mass. A heavy particle creates a peak in the resulting mass distribution, while background predominantly populates the low mass region. We present both a model-independent result for a single fiducial CHAMP, and a result interpreted within the context of a reference model for stable stop squark pair production. Since the leading order contributions to stop squark production depend only upon the stop mass [10], the result will generally apply to all stable stop production models.

To measure the velocity, we exploit the precision timing provided by the Time-of-Flight (TOF) detector [11] located at the perimeter of the tracking volume, augmented by additional timing information from the drift chamber (COT) [12]. Complete details of the CDF detector can be found in Ref. [13].

II. DATA SAMPLE & EVENT SELECTION

We search for CHAMPs in a data sample collected using a trigger that requires a single muon with a pseudo-rapidity [14] approximately in the range $|\eta| < 0.7$. The reconstructed muon must have $p_{\rm t} > 20$ GeV/c and pass quality criteria that reduce fakes and muons from decay-in-flight. No requirement is placed on the maximum energy in the calorimeter, as is typically the case to identify minimum ionizing muons. Cosmic rays, which are uncorrelated in time with respect to $\bar{p}p$ interactions and therefore present a potentially serious background, are removed by searching for evidence of an oppositely charged track opposite each muon track with $p_{\rm t} > 10$ GeV/c[15]. An event is rejected if such a pair is consistent with one inwardly-moving and one outwardly-moving track.

Figure 1 shows the distribution of the reconstructed $p_{\rm t}$ in MC data for stable stop squarks with masses of 100 GeV/c (blue) and 260 GeV/c^2 (red). The stop $p_{\rm t}$ distributions are typical for models of CHAMP production at CDF for masses within this range. Motivated by these distributions, we classify tracks with $p_{\rm t} > 40$ GeV/c as *signal region* tracks. The vast majority of CHAMPs with mass greater than 100 GeV/c^2 should fall into this category. Tracks with $20 < p_{\rm t} < 40$ GeV/c are *control region* tracks since they are dominated by $W \rightarrow \mu\nu$ decays and should be depleted in signal events. The remainder of the tracks, with $p_{\rm t} < 20$ GeV/c, are classified as t_0 tracks and are used to measure when the interaction occured.

We then define signal and control event samples by selecting muon events in which the leading muon triggered the detector, resides in the signal or control region, respectively, and points to the primary event vertex. From the signal sample, we select as CHAMP candidate tracks the leading muon track, and either the second leading muon or, if no second muon is present, the leading non-muon track. In both cases, the second candidate track must belong to the signal region and point to the same event vertex as the trigger muon. Similarly, a set of control tracks is isolated from the control sample using the same algorithm, except requiring the tracks to belong to the control region.

To identify a CHAMP signal among candidate tracks, we use the velocity and momentum to calculate the *TOF mass* of the candidate particle. The track velocity for all candidate and control tracks is measured by dividing the path length of the track by its time-of-flight (TOF). The TOF is measured by subtracting the event t_0 measured with

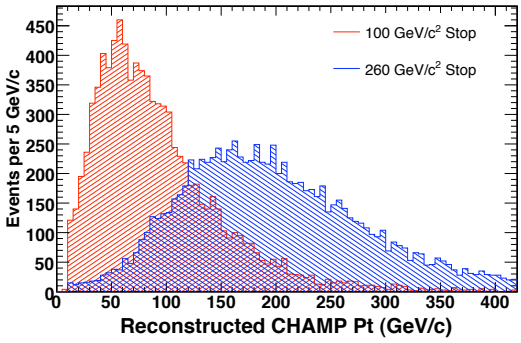

FIG. 1: Reconstructed transverse momentum (p_t) of stable stop squarks with masses of 100 GeV/c^2 (red) and 260 GeV/c^2 (blue) in MC data.

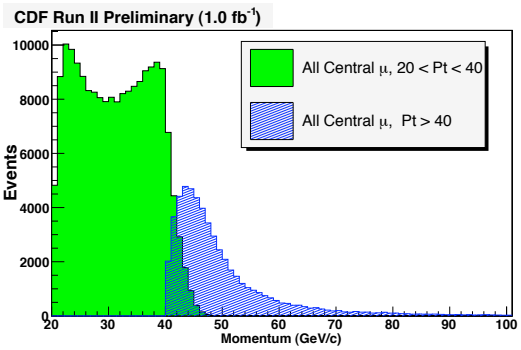

FIG. 2: Momentum distribution for candidate and control tracks.

the TOF detector using all t_0 tracks that point to the same vertex as the trigger muon, from the candidate's arrival time at the TOF detector. Non-Gaussian tails in the time resolution functions introduce a potentially large source of background of CHAMP candidates. Momentum mis-measurements also pose a potential source of background at high TOF mass. We therefore impose the following selection criteria to suppress this background.

The hit residuals to the track fit in the COT can be used to estimate the production time for all t_0 tracks independently of the TOF detector. While these measurements have about a factor of three worse resolution than those made with the TOF, they do not have significant non-Gaussian tails. The event t_0 and track velocity measurements from the TOF and COT must agree within uncertainties. We also exclude tracks that have a velocity close to c by requiring $\beta < 0.9$ as measured by the TOF. Finally, candidate tracks with anomalously large momentum, which are indicative of reconstruction errors, are rejected. Figure 2 shows the resulting momentum distributions for candidate and control tracks. The β distribution for candidate and control tracks are shown in Fig. 3

III. BACKGROUNDS

Since there are no CHAMPs in the standard model, background in the TOF mass distribution arises entirely from mis-measurements of the track velocity or momentum due to instrumental effects, or from incorrectly associating tracks with vertices that are unrelated. Errors in the velcity are dominated by mis-measurements in the event t_0 or the track arrival time. Cosmic rays that trigger the detector introduce a large source of tracks uncorrelated with $\bar{p}p$ collisions. Multiple interactions can also introduce errors in the track-vertex association or large t_0 errors, but these are well modeled in the time resolution function.

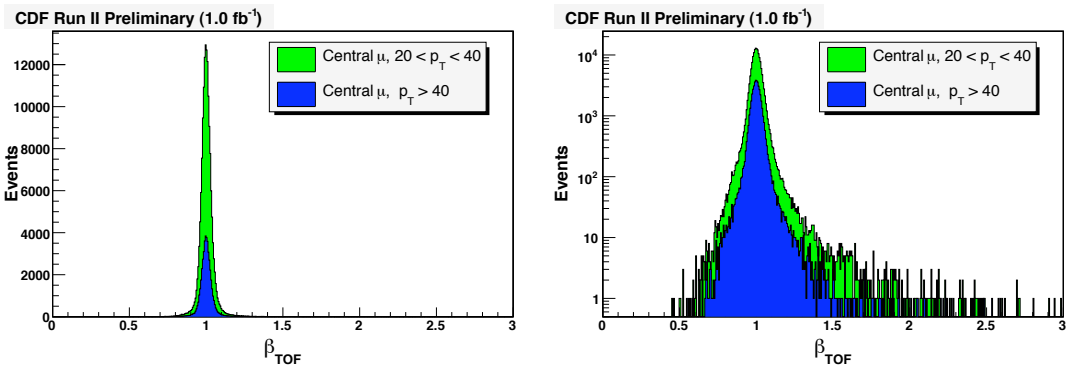

FIG. 3: Measured β distribution for candidate and control tracks.

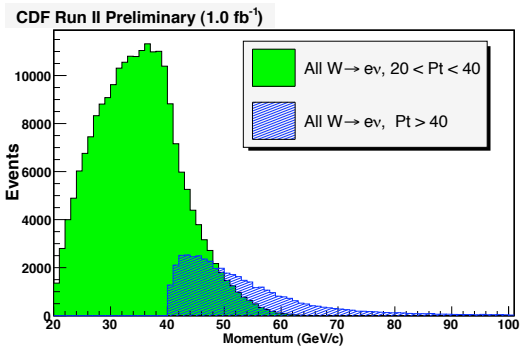

FIG. 4: Momentum distribution for control and signal region electrons in $W \rightarrow e\nu$ events.

A. Background from timing errors

The time resolution functions for t_0 and arrival time measurements are studied using well-identified $W \rightarrow e\nu$ events where we treat the electron track as the candidate or control track, as appropriate. We do not expect to find any real CHAMPs in this sample, so all electron tracks should have a measured $\beta \approx 1$.

In Figs. 4 and 5, we show the momentum and β distributions for control and signal region W electrons. It is evident that the shape of the TOF mass distribution will be determined primarily by the shape of the β distribution. If we assume that the error in the β measurement is independent of the momentum, then we can obtain an absolute prediction for the TOF mass distribution for a given set of tracks by convolving the track momentum distribution with the β distribution (actually, with the distibution of $\sqrt{1/\beta^2 - 1}$) for control tracks normalized to unit area. Figures 6 and 7 show the measured (histogram) and predicted (curve) TOF mass distribution for control and signal region W electron tracks. Both predictions use the shape of the β distribution for control region electrons. The agreement between the observed and predicted shapes confirms the hypothesis that β errors are largely uncorrelated with momentum, and verifies that we can predict the shape of the TOF mass distribution.

Since some features of the muon track sample differ from those of electron tracks (e.g., muons from decay-in-flight, bremstrahlung in the electron sample). it is important to check that the procedure also works within the muon sample. In Fig. 8, we show the observed and predicted TOF mass distribution for control muon tracks in which we have used the shape of the β distribution for control muons with $20 < p_{\rm t} < 30$ GeV/c and the momentum distribution for control muons with $30 < p_{\rm t} < 40$ GeV/c to predict the shape of the TOF mass distribution control muons with $30 < p_{\rm t} < 40$ GeV/c. We conclude that we can model the shape of the TOF mass distribution in the muon sample.

Note that since the control and signal samples in both the electrons and muons are selected from the same runs, the background checks above include all luminosity-dependent effects, such as multiple event overlaps, etc. The observed agreement between the measured and predicted background shows that these effects are well modeled by the above procedure.

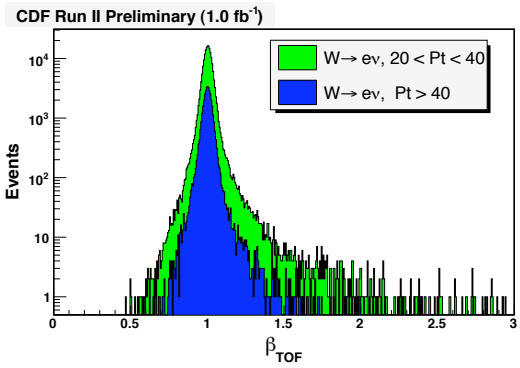

FIG. 5: The measured β distribution for control and signal region electrons in $W \to e\nu$ events.

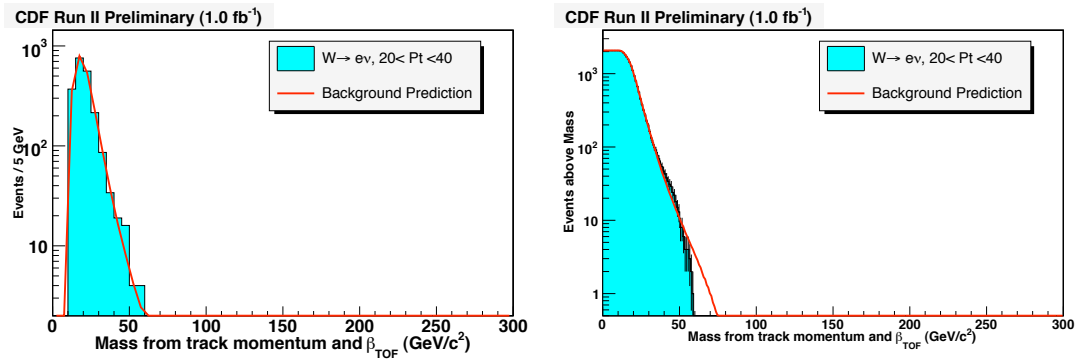

FIG. 6: Measured (histogram) and predicted (curve) TOF mass distribution for control region electrons in $W \to e\nu$ events. The plot on the right is the integral of the plot on the left from a given TOF mass upward.

B. Background from cosmic rays

To estimate the residual background from cosmic rays, we take a sample of about 600k events with cosmic ray muons tagged using the algorithm described in Sect. II. and pass them through the full analysis. Only three cosmic ray tracks survive and have a TOF mass greater than 100 GeV/c^2. Given that the cosmic ray filter rejects well over 99.9% of real cosmic rays, we conclude that there is negligible cosmic ray background with TOF mass greater than

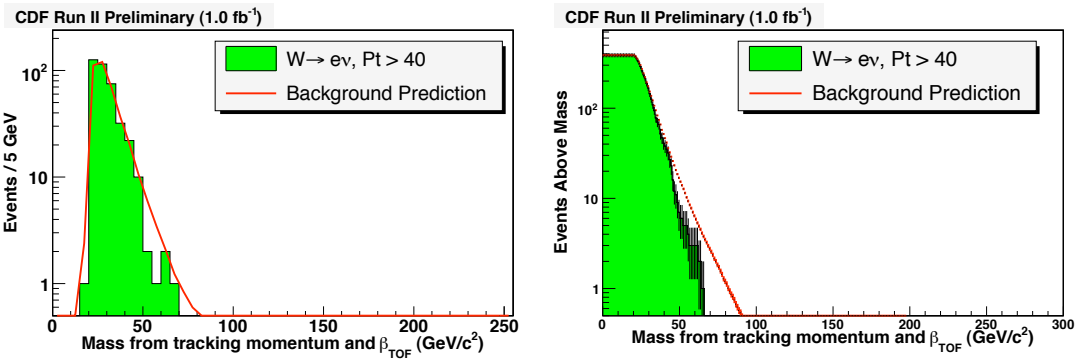

FIG. 7: Measured (histogram) and predicted (curve) TOF mass distribution for signal region electrons in $W \to e\nu$ events. The plot on the right is the integral of the plot on the left from a given TOF mass upward.

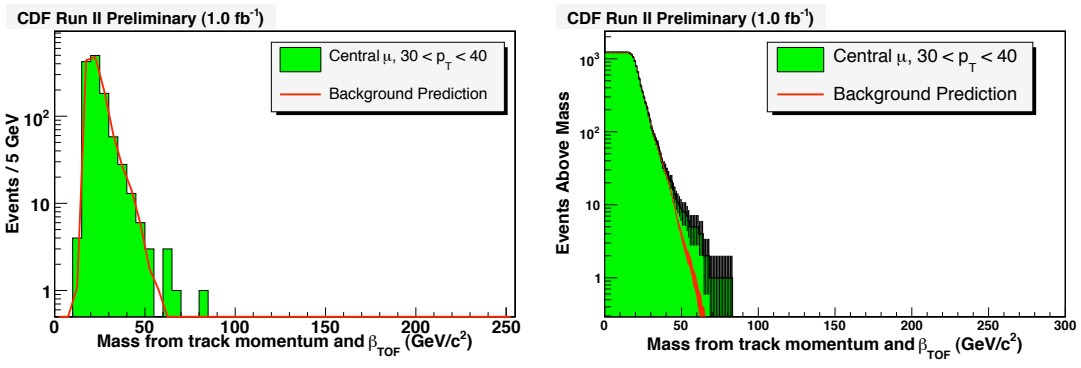

FIG. 8: Measured (histogram) and predicted (curve) TOF mass distribution for control muon tracks with $30 < p_{\rm t} < 40$ GeV/c. The predicted TOF mass distribution is obtained by using the β distribution for control muon tracks with $20 < p_{\rm t} < 30$ GeV/c convolved with the momentum distribution for control muons with $30 < p_{\rm t} < 40$ GeV/c. The plot on the right is the integral of the plot on the left from a given TOF mass upward.

100 GeV/c^2.

IV. EFFICIENCIES AND SYSTEMATIC UNCERTAINTIES

We estimate the efficiency for identifying a CHAMP candidate within the context of our reference model using a combination of data and Monte Carlo (MC). In general, CHAMPs are expected to have very large $p_{\rm t}$ and be highly isolated. Final state radiation is strongly suppressed, even in the case in which the CHAMP is strongly interacting [4]. These general characteristics make $W \rightarrow e\nu$ events a reasonable model for both the isolate CHAMP track and the underlying event. We therefore use $W \rightarrow e\nu$ events to estimate the efficiency for finding the primary event vertex and calculating an event t_0, and the decay electron tracks to estimate the efficiency for reconstructing an isolated CHAMP track associated with the vertex, and successfully measuring the arrival time at the TOF detector for tracks that are not fiducial to the muon detector. We use the muon data directly to determine the efficiency for measuring the arrival time for CHAMP tracks that are fiducial to the muon detector. Similarly, we use $Z \rightarrow \mu^+\mu^-$ events to measure the trigger efficiency for a single CHAMP track. The data-taking periods for the electron and muon datasets are identical so as to correctly model the effect of instantaneous luminosity on the efficiencies. To estimate the systematic uncertainties in these efficiencies, we include the statistical uncertainties of the measurements and, in the case of the arrival time efficiency, the difference between the efficiencies for electrons and muons, and a small drop in efficiency during the course of the run due to gain changes in the TOF system.

Strongly interacting CHAMPs are subject to QCD effects [4][5] that can reduce the overall detection efficiency relative to a weakly interacting. Quark-like CHAMPs, for instance, can hadronize into either charged or neutral color singlet states. Charge-exchange interactions in the material of the detector can change an initially charged singlet state into a neutral particle before reaching the muon detectors, and therefore before the detector is triggered.

To estimate the efficiency loss due to these hadronic effects in this analysis, we assume that a top squark hadronizes into a $\tilde{t}\bar{q}$ smeson state, neglecting a small fraction that hadronize into sbaryon $t\tilde{q}q$ states. The hadronization into a charged smesons is assumed to be (52.9±2.3)%, follow the rates for charged b-meson states as measured at LEP [16]. The center-of-mass energy for collisions between a massive squark moving at low velocity and a light quark is small. As a result, hadronic interactions within the material of the detector and the stop smeson involve primarily the light quark while the stop remains a spectator. We therefore assume the interaction length for the smeson to be one third of that for a proton. Under these assumptions, the probability that an initially charged stop smeson undergoes re-hadronization is 80% before the first muon detector and 63% between the first and second muon detectors. At each interaction, the stop re-hadronizes according to the same prescription as for the initial hadronization. To estimate the systematic uncertainty, we take the difference between the result above and the efficiency assuming that 100% of stop smesons re-hadronize.

Geometric and kinematic acceptances are calculated using Pythia modified to allow stable stop production. The trigger and detection efficiencies are calculated by combining the single track and vertex finding efficiencies as described above with the relative rate at which one or two stop smesons are fiducial to the to the detector and trigger as predicted by the MC. The systematic uncertainty includes the statistical uncertainties of these estimates and the correlations between the various event topologies.

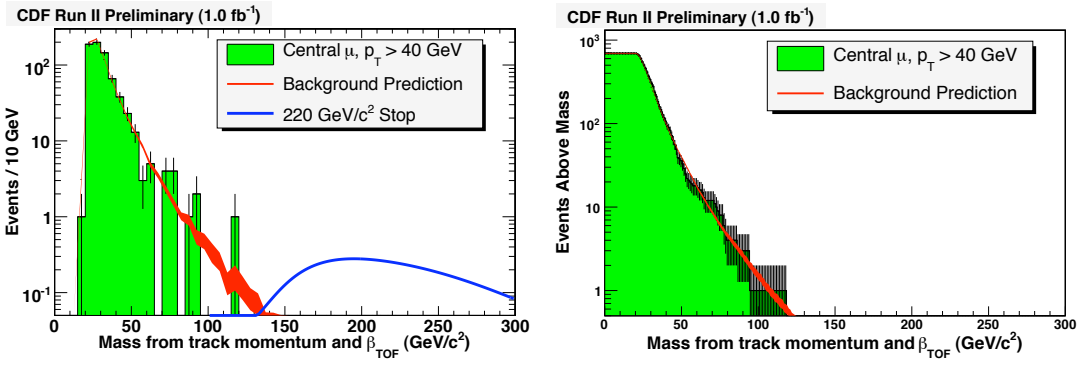

FIG. 9: Observed (histogram) and predicted (curve) TOF mass distribution for candidate tracks in the muon sample. The plot on the right is the integral of the plot on the left from a given TOF mass upward.

Stop mass (GeV/c^2)	100	120	140	160	180	200	220	240	260
Expected background	4.7±0.3	1.9±0.2	0.8±0.1	0.37±0.05	0.18±0.03	0.09±0.02	0.05±0.01	0.03±0.01	0.016±0.005
N observed	4	1	1	0	0	0	0	0	0
Effic × acceptance (%)	3.6±0.5	4.2±0.5	4.5±0.6	5.1±0.7	5.5±0.8	5.8±0.8	5.9±0.9	5.9±0.8	6.2±0.9
Expected limit (fb)	190	120	90	71	61	56	55	53	51
95% CL limit (fb)	160	90	100	60	56	53	52	52	50

TABLE I: Results of the search for stable stop squarks in 1.0 fb^{-1} of $\bar{p}p$ collisions, as a function of the stop mass.

V. RESULTS

Figure 9 shows the observed and predicted TOF mass distribution for signal region muons. We find one candidate muon with a TOF mass above 100 GeV/c^2 and none above 120 GeV/c^2, consistent with predicted background. From this result, we set a model-independent upper limit on the production cross section for a single, isolated, strongly interacting CHAMP fiducial to the muon trigger (approximately $|\eta| < 0.7$) with $p_t > 40$ GeV/c and $0.4 < \beta < 0.9$ to be $\sigma < 48$ fb at 95% C.L. Similarly, the cross section limit for a weakly interacting CHAMP under the same assumptions is $\sigma < 10$ fb at 95% C.L.

To count the number of events consistent with a stable stop of a given mass m_s, we must take into account the resolution of the TOF mass measurement. We therefore integrate all events within a one-sided window from $0.8m_s$ upward. Table I shows the number of observed and predicted events as a function of the stop mass. From the efficiencies in the previous section and the expected background, we estimate the expected cross section limit as a function of the stop mass shown in Fig. 10. The observed 95% C.L. upper limit on the cross cross section is shown in Fig. 11. The theoretical NLO stop production cross section, as calculated using the Prospino2 program [17], is represented by the red curve. From the intersection of these two curves, we infer a 95% C.L. upper limit on the mass of a stable stop to be 250 GeV/c^2, which coincides with the expected mass limit.

Acknowledgments

We thank the Fermilab staff and the technical staffs of the participating institutions for their vital contributions. This work was supported by the U.S. Department of Energy and National Science Foundation; the Italian Istituto Nazionale di Fisica Nucleare; the Ministry of Education, Culture, Sports, Science and Technology of Japan; the Natural Sciences and Engineering Research Council of Canada; the National Science Council of the Republic of China; the Swiss National Science Foundation; the A.P. Sloan Foundation; the Bundesministerium fuer Bildung und Forschung, Germany; the Korean Science and Engineering Foundation and the Korean Research Foundation; the Particle Physics and Astronomy Research Council and the Royal Society, UK; the Russian Foundation for Basic Research; the Comision Interministerial de Ciencia y Tecnologia, Spain; and in part by the European Community's

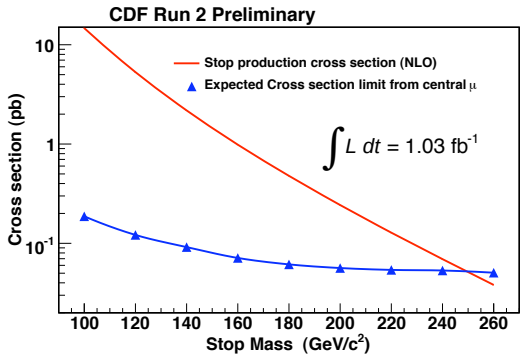

FIG. 10: Expected 95% C.L. cross section limit for the production of stable stop squarks for this analysis (blue points). The theoretical NLO cross section as calculated by the Prospino2 program is shown in red. Based upon the intersection of these curves, the expected mass limit for a stable stop is 250 GeV/c^2.

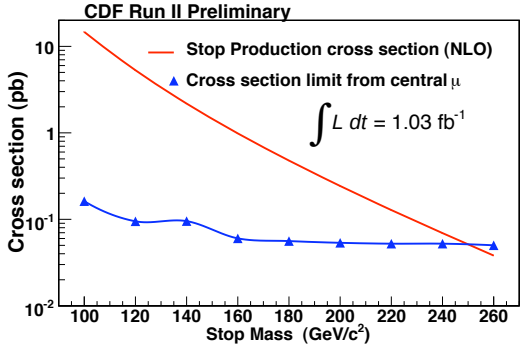

FIG. 11: The observed 95% C.L. cross section limit for the production of stable stop squarks (blue points). The theoretical NLO cross section as calculated by the Prospino2 program is shown in red. The intersection of these two curves yields a lower mass limit for a stable stop of 250 GeV/c^2.

Human Potential Programme under contract HPRN-CT-20002, Probe for New Physics.

[1] See R. Barbieri, L. J. Hall and Y. Nomura, Phys. Rev. D **63**, 105007 (2001); T. Appelquist, H. C. Cheng and B. A. Dobrescu, Phys. Rev. D **64**, 035002 (2001)
[2] See for instance P.H. Frampton and P.Q. Hung, Phys. Rev. D **58**, 057704 (1997); M. Dine, A. E. Nelson and Y. Shirman, Phys. Rev. D **51**, 1362 (1995); M. Dine *et al.*, Phys. Rev. D **53**, 2658 (1996); N. Arkani-Hamed and S. Dimopoulos, JHEP **0506**, 073 (2005).
[3] J. L. Feng *et al.*Phys. Rev. Lett. **83**, 1731 (1999) J. L. Feng and T. Moroi, Phys. Rev. D **61**, 095004 (2000)
[4] M. Drees and X. Tata, Phys. Lett. B **252**, 695 (1990).
[5] M. Fairbairn *et al.*, Phys. Rept. **438**, 1 (2007).
[6] P. F. Smith *et al.*, Nucl. Phys. B **206**, 333 (1982); M. Byrne, C. F. Kolda and P. Regan, Phys. Rev. D **66**, 075007 (2002).
[7] F. Acosta *et al.*, Phys. Rev. Lett. **90**, 131801 (2003).
[8] A. Heister *et al.* [ALEPH Collaboration], Phys. Lett. B **537**, 5 (2002).
[9] LEPSUSYWG, ALEPH, DELPHI, L3 and OPAL experiments, note LEPSUSYWG/02-05.1 (http://lepsusy.web.cern.ch/lepsusy/Welcome.html).
[10] W. Beenakker *et al.*, Nucl. Phys. B **515**, 3 (1998); E. L. Berger, M. Klasen and T. Tait, Phys. Rev. D **59**, 074024 (1999).
[11] C. Paus *et al.*, Nucl. Instrum. Meth. A **461**, 579 (2001); C. Grozis *et al.*, Nucl. Phys. Proc. Suppl. **93**, 344 (2001); C. Grozis *et al.*, Int. J. Mod. Phys **A16S1C**, 1119 (2001); S. Cabrera *et al.*, Nucl. Instrum. Meth. A **494**, 416 (2002).
[12] T. Affolder *et al.*, Nucl. Instrum. Meth. **526**, 249 (2004).
[13] D. Acosta *et al.*, Phys. Rev. D **71**, 032001 (2005).

[14] The pseudo-rapidity, η, is defined by $\eta = -\log\tan(\theta/2)$, where θ is the polar angle measured with respect to the proton direction.
[15] A. V. Kotwal, H. K. Gerberich and C. Hays, Nucl. Instrum. Meth. A **506**, 110 (2003).
[16] E. Barberio *et al.* [Heavy Flavor Averaging Group (HFAG) Collaboration], arXiv:0704.3575 [hep-ex].
[17] See Tilman's Official Prospino page for details. The calculation for stop pair production is based upon Ref. [10].